Available online at www.sciencedirect.com

ScienceDirect

IFAC PapersOnLine 56-2 (2023) 10051–10056

Dynamic Analysis of the Italian Gas Distribution Network

Jan Hämmelmann * **Matteo Luigi De Pascali** * **Francesco Casella** *

* *Politecnico di Milano, Dipartimento di Elettronica, Informazione e Bioingegneria, 20133 Milano, Italy (e-mail: matteoluigi.depascali,francesco.casella@polimi.it, jan.hammelmann@mail.polimi.it)*

Abstract: In this work, a dynamic analysis of a natural gas distribution network is performed exploiting a flexible Modelica framework. The case study focuses on the Italian grid with the aim of providing useful indications for optimization tasks. Through linearization and model order reduction, a simplified model of the network is obtained to evaluate the governing time constants with which pressures propagate along the network after rotational speed changes of the compression stations. Further indications are provided regarding compression stations mutual interactions. The analysis is validated considering simplified network models and specific tests on the entire network. The proposed approach can also be applied to systems of comparable size and complexity that can transport hydrogen and hydrogen mixtures.

Keywords: Dynamic Analysis, Linearization, Gas Networks, Modelica

1. INTRODUCTION AND OBJECTIVES

According to IEA (2019), natural gas will play an important role in the transition period towards the net zero emissions goal. Recent events have also changed market shares and suppliers from which European countries, relying on natural gas, import this fuel. Moreover, the continuous increase of its price influences dramatically storage campaigns. Thus, a safe and efficient transportation grid operation is a necessary practice to prevent disservices and reduce operative costs. Nonetheless, natural gas grids can serve also as an infrastructure to develop a hydrogen economy, since pipelines are suited to transport natural gas-hydrogen mixtures (see Melaina et al. (2013)).

In this paper, starting from the framework proposed by the same authors (see De Pascali et al. (2022)), a small-signal dynamic analysis of a natural gas transportation network is performed in frequency and time domains. The aim of the analysis is to understand the dynamic behaviour of such system reacting to changes in the rotational speed of the compressors to regulate pressures and mass flow rates along the grid. This task is accomplished through a graphical representation of pressures evolution displayed directly on the map of the network. The case study is the same as in the previous work (i.e. the Italian high pressure gas distribution network).

Differently from what happens for electrical distribution networks, which are strongly coupled and react to inputs and disturbances in seconds, natural gas grids operate on totally different time scales. Knowing which are the time constants of interest is thus essential to design effective control and optimization strategies for activities like the one described in the paper by Ghilardi et al. (2022).

The main contribution of this paper is twofold. On one hand, it presents a modelling framework that allows to spatially visualize the frequency- and time-domain dynamic response of a large gas network to its main manipulated variables, i.e., the compressor speeds. On the other hand, it presents the results of this analysis when applied to the Italian natural gas transportation network, which is one of the world's largest, managed by a single operator.

The results of this activity can be useful in view of optimal control of the network operation with direct numerical methods: being able to provide indications on possible dynamic decoupling of grid areas and suggestions on the different effects that stations have on the network may help simplifying the optimization problem.

Thanks to the flexibility and re-usability of the employed framework, this analysis is not limited to the case study presented, but it can be performed on different configurations of the same grid and ideally on any network modelled through the same framework.

The tools used in this work are the Modelica language interpreted by OpenModelica (see Mattsson et al. (1998) and Fritzson et al. (2020)) to simulate and linearize the system, Matlab for the linearized model manipulation and analysis and Python to visualize the obtained results.

2. METHODOLOGY

The dynamic analysis object of this paper focuses on the Italian high-pressure natural gas distribution network. This grid has a total pipe length of approx. 8000 km, it features about 1800 pipes and 6000 nodes and comprises 15 compression stations. To model such a large, complex and integrated network De Pascali et al. (2022) employed a graph representation and a simplification algorithm to

Peer review under responsibility of International Federation of Automatic Control.
10.1016/j.ifacol.2023.10.873

translate the network dimensional and operating data into a Modelica model. This paper utilizes the same framework and analyzes the entire network taking input data of a day of operation from year 2021.

Since the network never reaches a steady-state during real operation, the non-linear system representing the network should in principle be linearized around an operating trajectory, resulting in a time-variant linearized system, the main sources of non-linear behaviour being the friction losses (which are quadratic with the flow rate) and the compressor operating maps. However, the operating point seldom changes drastically within a 24-48 hours horizon, so the analysis of the system dynamics performed at a specific time instant over such a time horizon still provides very valuable insight into the system dynamic behaviour. Results shown in section 3 support this assumption.

At the system boundaries, certain mass flow rates are prescribed, corresponding to imports/exports from/to the adjacent network, to flows to/from the underground storage systems and to flows to consumers. These flows are determined by market operators and by consumers and are thus given exogenous inputs for the network operator.

On the other hand, compressor stations inside the network are operated by local controllers, that adjust the compressor speeds following the one set point among station mass flow rate, minimum inlet pressure and maximum outlet pressure, that leads to the minimum rotational speed request; the last two set points act as safety limitations, see De Pascali et al. (2022) for more details. These set-points are decided in real-time by the network operator.

For the ultimate goal of global system optimization, however, it is convenient not to consider these local controllers, that introduce very strong nonlinear behaviour in the system dynamics, but rather to assume the compressor speeds as the manipulated variables, with upper and lower pressure limits being enforced during optimization by box constraints, which are fundamentally easier to manage.

To linearize the system using those rotational speeds as inputs, the original model is simulated twice. A first simulation is run with local controllers following recorded set points from operation databases, obtaining the normalized rotational speed trajectories $N^0(t)$. Then, a second simulation is run without those controllers, by directly applying $N^0(t) + \Delta N(t)$ to the compressor speeds, $\Delta N(t)$ being additive infinitesimal perturbations to consider as inputs for linearization. The considered outputs are the pressures at the pipe inlets and outlets.

The OpenModelica tool automatically generates a state-space representation of the system dynamics, from which it can compute the A, B, C, D matrices by numerical and symbolic differentiation methods, applied at a specific point in time. Since the full network model accounts for more than 700 states, linear model order reduction is performed to reduce the computational effort in the subsequent analysis, using Matlab's balanced order reduction *balred()* function. This transforms the state space-representation into a system characterized by equal observability and controllability Gramians, with states ranked by their singular values. A reduced-order system is obtained by retaining the first n_r states that have the bigger singular values, choosing n_r so that the response of the reduced system does not differ significantly from the one of the original model on the time scale of interest, from 1 hour to one or two days.

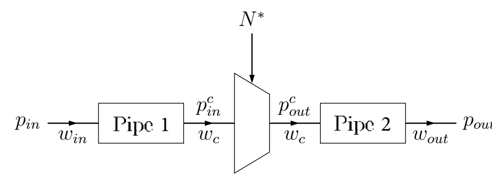

Fig. 1. Scheme topology 1

The reduced-order linearized system can then be analyzed in the time (step response) or frequency (frequency response) domains and mapped onto a diagram that shows the spatial distributions of the outputs of interest.

3. VALIDATION

The developed toolchain was first validated with simple models, for which linearized transfer functions can be computed analytically. Results are shown in this Section.

3.1 Topology 1

In this configuration (see figure 1) a compressor is placed between two pipes, with prescribed mass flow rates w_{in} and w_{out} at the system boundary and no distributed consumption along the pipes. The compressor model reads:

$$H = c_1 + c_2Q + c_3N + c_4NQ + c_5Q^2 + c_6N^2 \tag{1}$$

$$(h^c_{out} - h^c_{in}) = k_1 + k_2p^c_{out} + k_3p^c_{in} + k_4p^c_{out}p^c_{in} + k_5{p^c_{out}}^2 + k_6{p^c_{in}}^2, \tag{2}$$

where H and Q are compressor head and volumetric flow rate, N is the normalized rotational speed, h^c and p^c are specific enthalpies and pressures referred to the compressor, c_i and k_i are constant coefficients. Linearizing equations (1) and (2), the following expressions are obtained:

$$\Delta H = B_Q\Delta Q + B_N\Delta N \tag{3}$$

$$\Delta(h^c_{out} - h^c_{in}) = E_o\Delta p^c_{out} + E_i\Delta p^c_{in}, \tag{4}$$

where B_Q, B_N, E_o and E_i are constant coefficients deriving from the linearization process. Since relations (5) and (6) hold and by neglecting the variations of inlet gas density for simplicity, equation (7) is obtained, where g is the acceleration of gravity:

$$Hg = h^c_{out} - h^c_{in} \tag{5}$$

$$\Delta Q = \frac{\Delta w}{\rho_{in}} \tag{6}$$

$$\left(\frac{B_Q}{\rho_{in}}\Delta w_c + B_N\Delta N\right) g = E_o\Delta p^c_{out} + E_i\Delta p^c_{in} \tag{7}$$

By introducing the same hypothesis from De Pascali et al. (2022), pipes are modelled through the telegraph equation with the formulations reported in equations (8) and (9). The transfer matrices contain suitable transcendental transfer functions based on the formulation reported by Peres et al. (1998).

$$\begin{bmatrix}\Delta p_{in}\\ \Delta w_{in}\end{bmatrix} = \begin{bmatrix}A^{p1}_{11}(s) & A^{p1}_{12}(s)\\ A^{p1}_{21}(s) & A^{p1}_{22}(s)\end{bmatrix}\begin{bmatrix}\Delta p^c_{in}\\ \Delta w_c\end{bmatrix} \tag{8}$$

$$\begin{bmatrix}\Delta p^c_{out}\\ \Delta w_c\end{bmatrix} = \begin{bmatrix}A^{p2}_{11}(s) & A^{p2}_{12}(s)\\ A^{p2}_{21}(s) & A^{p2}_{22}(s)\end{bmatrix}\begin{bmatrix}\Delta p_{out}\\ \Delta w_{out}\end{bmatrix} \tag{9}$$

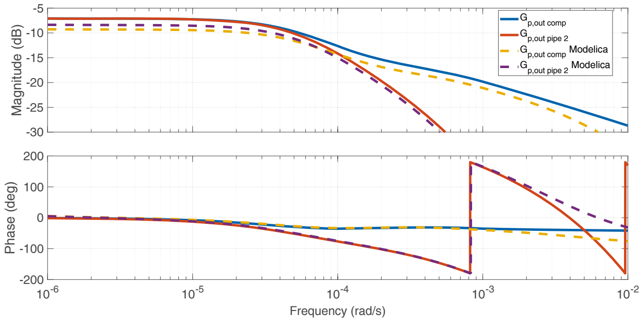

Fig. 2. Bode plot topology 1

Considering fixed boundary flow rates $\Delta w_{in} = \Delta w_{out} = 0$, the following transfer functions are obtained:

$$G^c_{out}(s) = \frac{\Delta p^c_{out}(s)}{\Delta N(s)} = \frac{-A^{p2}_{11} A^{p1}_{21} B_N g \overline{\rho_{in}}}{A^{p1}_{21} A^{p2}_{21} B_Q g + A^{p2}_{21} A^{p1}_{22} E_i \overline{\rho_{in}} - A^{p2}_{11} A^{p1}_{21} E_o \overline{\rho_{in}}} \tag{10}$$

$$G_{out}(s) = \frac{\Delta p_{out}(s)}{\Delta N(s)} = \frac{-A^{p1}_{21} B_N g \overline{\rho_{in}}}{A^{p1}_{21} A^{p2}_{21} B_Q g + A^{p2}_{21} A^{p1}_{22} E_i \overline{\rho_{in}} - A^{p2}_{11} A^{p1}_{21} E_o \overline{\rho_{in}}} \tag{11}$$

The frequency responses of these analytical transfer functions can be compared with those obtained from the linearization of the equivalent Modelica model, see figure 2. The results are satisfactory: the offset between the analytical solutions and the numerical ones is caused by the assumption of constant density in the analytical case. Discrepancies at high frequency are due to the approximations of the finite-volume numerical model, with respect to the infinite-dimensional analytical one.

3.2 Topology 2

The gas network model can contain loops connecting the inlet and the outlet of a compressor. Topology 2 (see figure 3) is analyzed to show what is the behaviour of such a system and how it compares with *topology 1*. The analytical expressions of the transfer functions are omitted for brevity in this case.

One of the main differences from the previous case lies in the change of mass flow rate processed by the station after a step increase of the compressor speed. Once the transient is over, in *topology 1* the flow rate returns to its original value, while for *topology 2* the loop flow rate is increased, leading to a steady-state increase of the compressor flow rate (see figure 4).

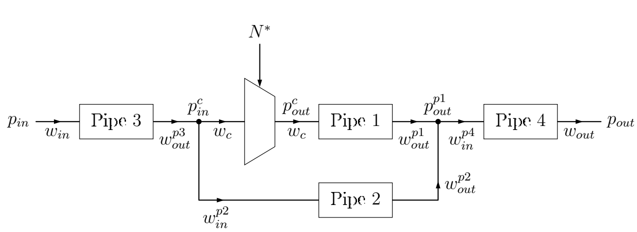

Fig. 3. Scheme topology 2

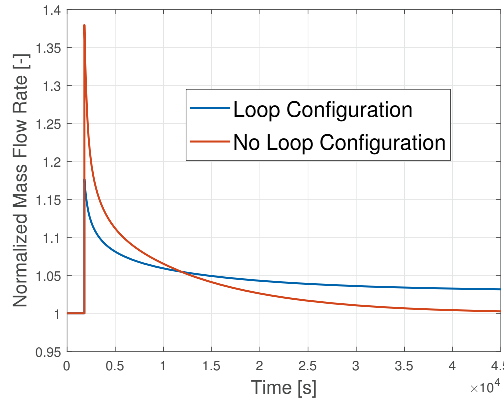

Fig. 4. Mass flow rates: topology 1 vs topology 2

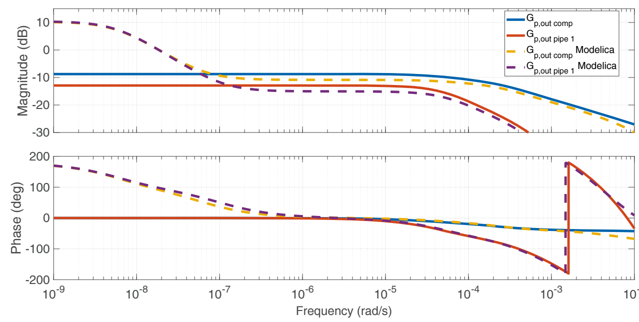

Fig. 5. Bode plot topology 2

As in the previous case, the Bode plots in figure 5 show a good agreement above $4 \cdot 10^{-7}$ rad/s, except for the offset due to the effect of changing density at the compressor inlet. However, at lower frequency, the Modelica model presents a significant gain and phase difference. This behaviour is due to an additional internal feedback in the Modelica model, caused by the change of fuel consumption of the compressor unit when the rotational speed is changed, an effect which was not considered in the analytical model. This leads to a significant change of the pipe pressures over a time scale that is considerably slower than the ones that are considered in this analysis, i.e. several weeks or months, so it is not relevant for the analysis presented here.

3.3 Italian network

The scenario on which the analysis is performed features four active stations (see figure 6). Malborghetto station is located near the border of the network, so its rotational speed cannot be considered as an input for the linearization; rather, its mass flow rate is prescribed to match the set point dictated by the market transactions with upstream providers. Applying the procedure described in Section 2, the model of the network is linearized considering as input the rotational speed of Poggio Renatico, Montesano and Messina stations.

The frequencies of interest for the dynamic analysis are between $\omega_{min} = 3 \cdot 10^{-6}$ rad/s and $\omega_{max} = 3 \cdot 10^{-3}$ rad/s (from 5 minutes to 4 days) and the selected order n_r for the model order reduction is 50. To check if the reduced order system still represents accurately the network behaviour,

Fig. 6. Grid with active stations for the analyzed scenario

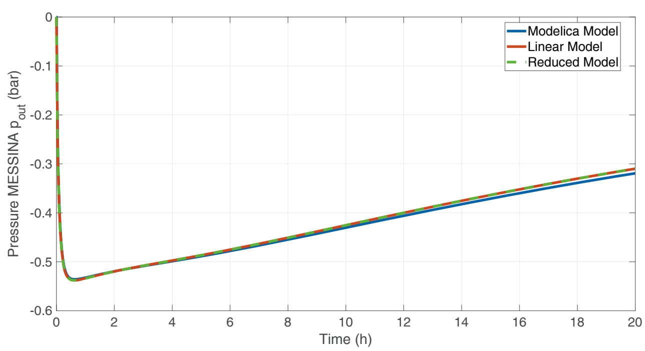

Fig. 7. Messina station outlet pressure after compressor speed step reduction in the same station

step tests are performed to compare the responses of the Modelica system and the linearized one.

Figures 7 and 8 show the effects of a step $\Delta N = -0.02$ on the normalized rotational speed at the Messina compression station on the outlet pressures of Messina and Montesano stations. The results obtained with the full nonlinear model, with the full linearized model and with the order-reduced model are virtually indistinguishable. Note how the effect of the speed reduction in Messina starts to be felt at Montesano, which is about 350 km away, with a delay of about 2 hours.

As mentioned in Section 2, the system never reaches steady state conditions and can be linearized along a defined system trajectory; to check if the time instant in which the linearization is performed significantly affects the analysis, the model was linearized at 5:00, 10:00, 15:00 and 20:00 of the considered day of operation. Figure 9 shows the Bode plots of the transfer function between the compressor speed in Messina and the outlet pressure in Montesano, computed in those four different time instants, which turn out to be nearly identical. This justifies the assumption that a linear, time-invariant approximation is good enough to understand the network dynamics over one/two days of operation.

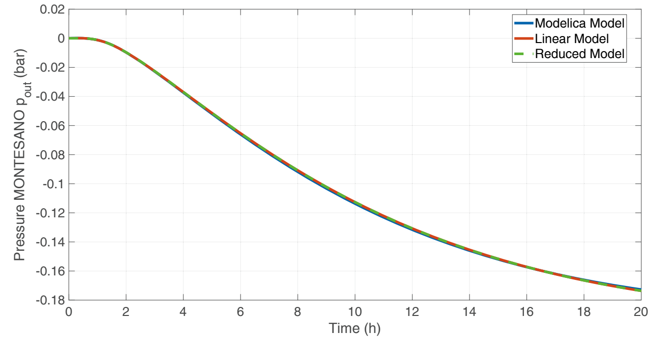

Fig. 8. Montesano station outlet pressure after compressor speed step reduction at Messina station

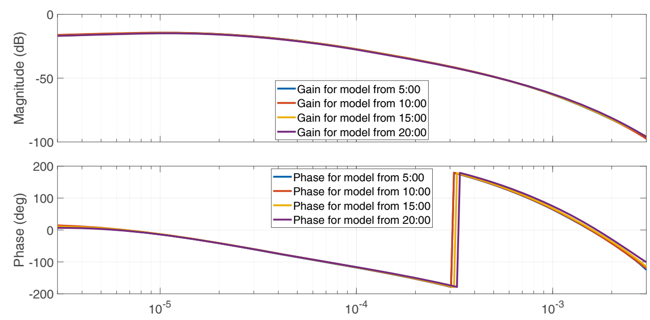

Fig. 9. Comparison of frequency responses at different points in time: transfer function between Messina rotational speed and Montesano outlet pressure

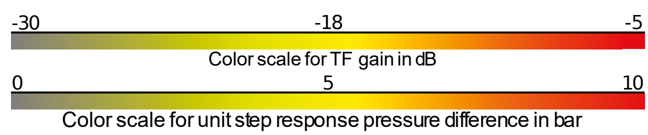

Fig. 10. Color scales for frequency and time domain analysis

4. RESULTS

In this section, the results of the dynamic analysis will be presented. The transfer function between the compressor speed changes and the pressure changes at each node are considered, since the main control objective of the network operator is to maintain an acceptable pressure distribution across the network, eventually trying to minimize the fuel consumption and associated emissions.

The pressure evolution is directly plotted on the network map at different points in time or frequency. Specifically, the color of each pipe represents the absolute value of the amplitude of the step response after a certain elapsed time or the magnitude of the frequency response at a certain frequency, respectively, averaged between the two pipe end nodes. The values follow the color scales shown in figure 10. This allows to clearly visualize how a specific compressor speed change gradually affects larger areas in the network as the time increases, or the frequency decreases.

Figure 11 shows the propagation of the effect of changes in the Messina compressor speed on the network pressure at different frequencies. At frequencies corresponding to 1.5 and 3 hours, the effect is mainly limited to Sicily and Calabria, eventually spreading to Northern Italy on

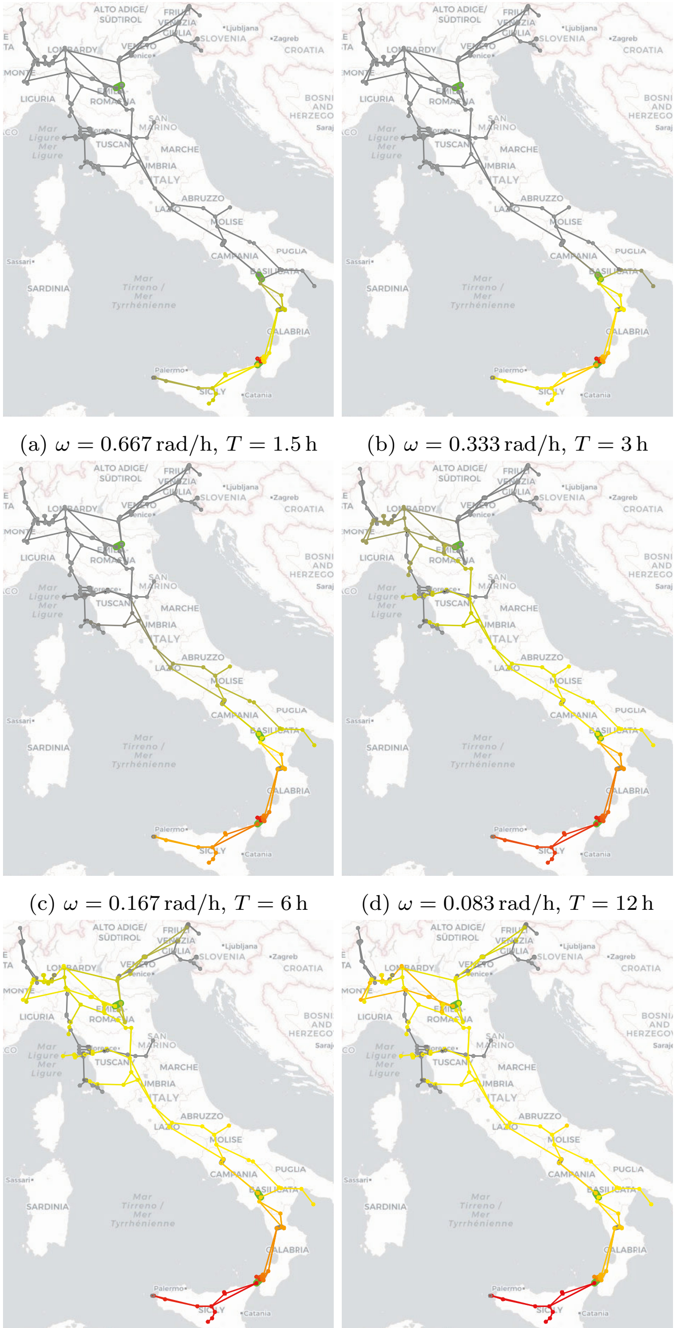

(a) $\omega = 0.667\,\mathrm{rad/h}$, $T = 1.5\,\mathrm{h}$ (b) $\omega = 0.333\,\mathrm{rad/h}$, $T = 3\,\mathrm{h}$

(c) $\omega = 0.167\,\mathrm{rad/h}$, $T = 6\,\mathrm{h}$ (d) $\omega = 0.083\,\mathrm{rad/h}$, $T = 12\,\mathrm{h}$

(e) $\omega = 0.042\,\mathrm{rad/h}$, $T = 24\,\mathrm{h}$ (f) $\omega = 0.021\,\mathrm{rad/h}$, $T = 48\,\mathrm{h}$

Fig. 11. Compressor speed change in Messina: freq. domain

frequency horizons corresponding to 24 hours or more. Some parts of the network remain unaffected, since they are located behind pressure reducing valves with fixed outlet pressure set point. The effect remains stronger upstream in Sicily, since that part of the network has a much lower volume than the downstream part. On the other hand, a fairly strong effect is visible in North-West Italy at the slower frequency, stronger than the effect in Central Italy. This apparently counter-intuitive behaviour is due to the amplification effect of the Poggio Renatico compression station, which increases its outlet pressure more than its inlet pressure increases, given enough time to do that. Among other things, these observations are relevant for optimization tasks, suggesting to a choice of

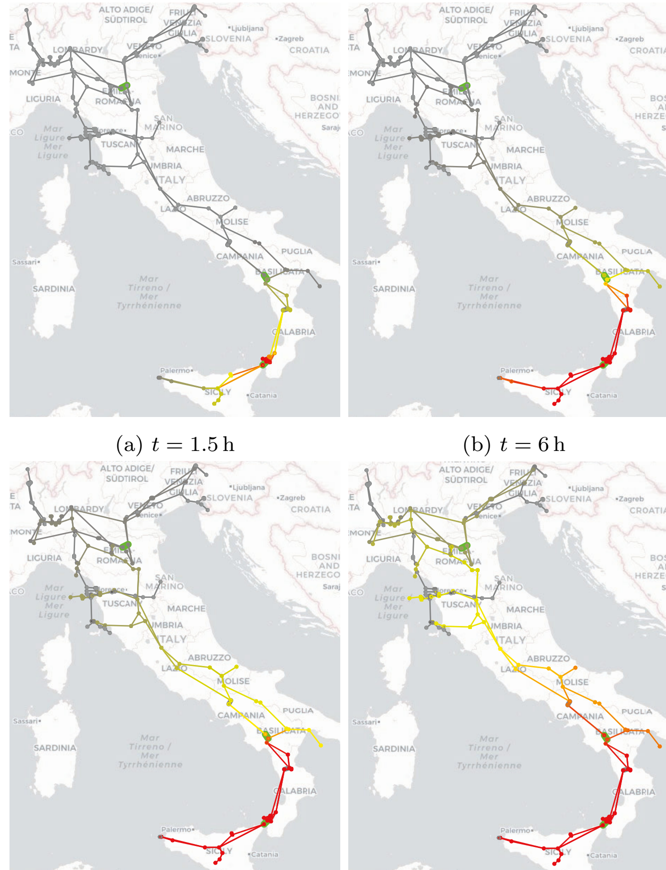

(a) $t = 1.5\,\mathrm{h}$ (b) $t = 6\,\mathrm{h}$

(c) $t = 12\,\mathrm{h}$ (d) $t = 24\,\mathrm{h}$

Fig. 12. Speed change in Messina: time domain

sampling time for collocation methods between one and two hours and a prediction horizon of at least 24 hours.

Figure 12 shows the time-domain propagation of the response to a step change in the Messina compressor speed. The behaviour in terms of areas of influence at different time scales is similar to that resulting from the frequency-domain analysis. Figure 13 shows the areas of influence of the nearby Montesano station, which are shifted toward North, compared to those of the Messina station.

Figure 14 highlights the presence of a closed loop over Northern Italy connected to the outlet of Poggio Renatico station. The pressures in this area are strongly affected after about 6 hrs, while the spillover towards the southernmost part of the network is quite limited. The sphere of influence of this compression station is quite apparent from this figure.

As a final remark, there are 15 available compression stations around the country, with the areas of influence of nearby stations overlapping significantly even over relatively short time periods (between 1.5 h and 3 h). When tackling the optimal unit commitment problem, which has a combinatorial complexity, one could reduce the size of the configuration space by excluding a priori that stations having similar effects on the grid are activated at the same time, thus saving the optimizer the evaluation of unnecessary scenarios.

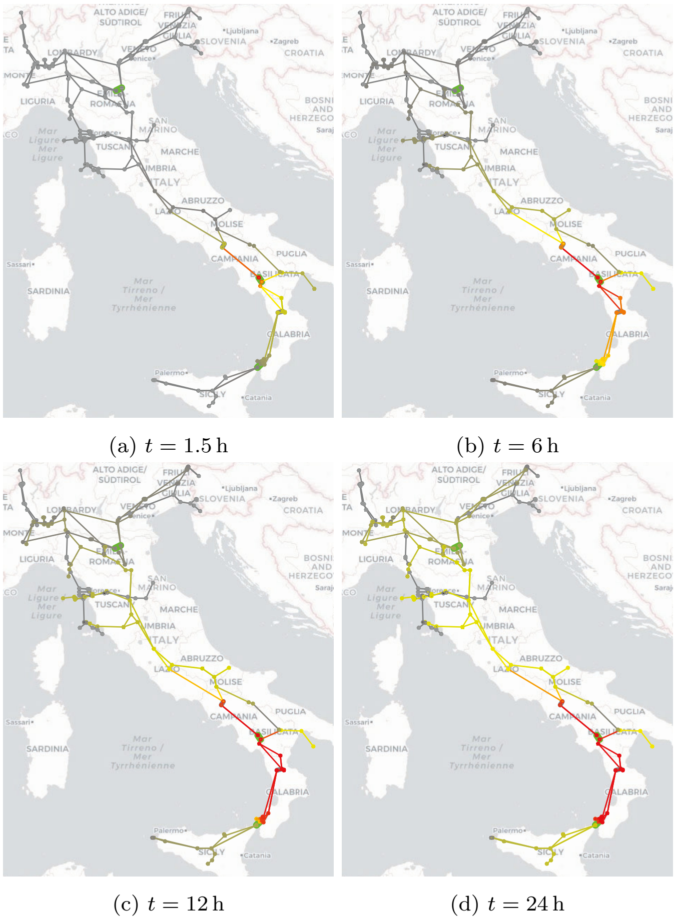

(a) $t = 1.5\,\mathrm{h}$ (b) $t = 6\,\mathrm{h}$

(c) $t = 12\,\mathrm{h}$ (d) $t = 24\,\mathrm{h}$

Fig. 13. Speed change in Montesano: time domain

5. CONCLUSION

In this paper, the framework from De Pascali et al. (2022) is exploited to perform a control-oriented dynamic analysis of the Italian high pressure natural gas distribution network, with the ultimate goal of supporting the set-up of a decision support system for the network operator based on network-wide optimal control.

The proposed methodology and toolchain are first validated through simplified tests comparing numerical and analytical results, then applied to the analysis of the network dynamic response during a recorded day of operation in 2021. Results can be visualized on maps, showing the areas of influence of the active compression stations over different time or frequency scales.

This information can provide valuable insights on the control-relevant dynamic behaviour of the system, in terms of time scales, areas of influence and coupling of the effects of different compression stations. This can be useful to support fully conscious design choices when tackling the optimal control problem of the network. For example, the analysis showed that a sampling time of 1-2 hours is likely fast enough, while an optimization horizon of at least 24 hours is necessary to fully capture the dynamic response of the overall system.

The proposed methodology is applicable to any gas transportation network of comparable size and complexity, including grids suitable for hydrogen and hydrogen-natural gas mixtures.

ACKNOWLEDGEMENTS

The authors are grateful to Snam S.p.A. for providing the data used in this paper.

REFERENCES

De Pascali, M.L. et al. (2022). Flexible object-oriented modelling for the control of large gas networks. *IFAC-PapersOnLine*, 55(9), 315–320.

Fritzson et al. (2020). The OpenModelica integrated environment for modeling, simulation, and model-based development. *Modeling, Identification and Control*, 41(4), 241–295.

Ghilardi, L.M.P. et al. (2022). A milp approach for the operational optimization of gas networks. *IFAC-PapersOnLine*, 55(9), 321–326.

IEA (2019). The role of gas in today's energy transitions.

Mattsson, S.E., Elmqvist, H., and Otter, M. (1998). Physical system modeling with modelica. *Control Engineering Practice*, 6(4), 501–510.

Melaina, M.W., Antonia, O., and Penev, M. (2013). Blending hydrogen into natural gas pipeline networks: a review of key issues.

Peres, P.L., Bonatti, I.S., and Lopes, A. (1998). Transmission line modeling: A circuit theory approach. *Siam Review*, 40(2), 347–352.

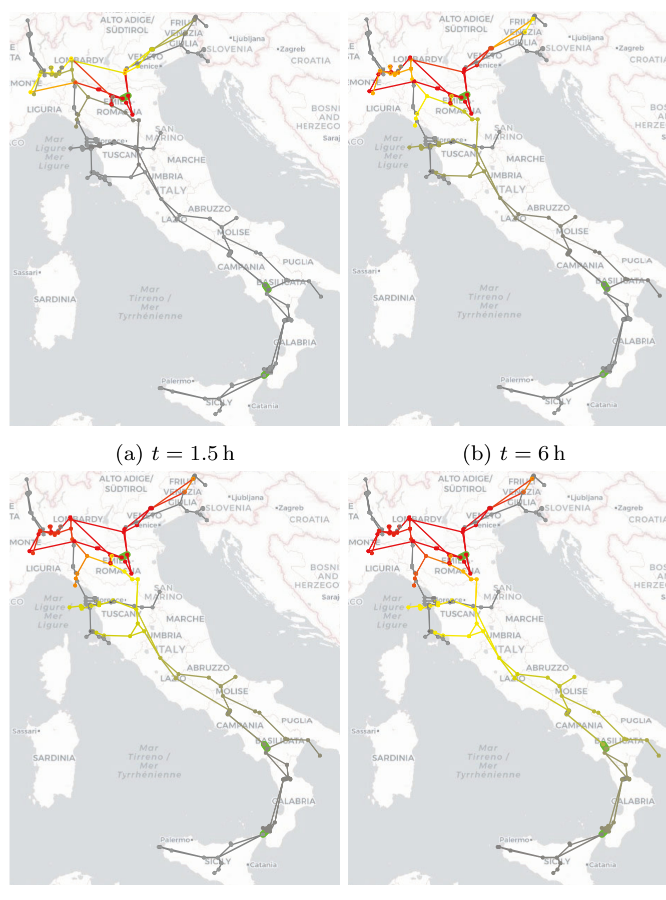

(a) $t = 1.5\,\mathrm{h}$ (b) $t = 6\,\mathrm{h}$

(c) $t = 12\,\mathrm{h}$ (d) $t = 24\,\mathrm{h}$

Fig. 14. Speed change in Poggio Renatico: time domain